International Journal of Advanced Engineering Research and Science (IJAERS)
Peer-Reviewed Journal
ISSN: 2349-6495(P) | 2456-1908(O)
Vol-12, Issue-11; Nov, 2025
Journal Home Page Available: https://ijaers.com/
Article DOI: https://dx.doi.org/10.22161/ijaers.1211.6

A Programmable Multi-Voltage Battery Charger using PIC16F877A: Proteus-Based Design and Simulation for Renewable Energy Applications

Sylvester Tirones[1, *], Yue Hu[2]

[1]Department of Electrical Engineering, Shanghai Jiao Tong University, China
Email: stirones@sjtu.edu.cn
[2]Department of Electrical Engineering, Shanghai Jiao Tong University, China
Email : yuehu@sjtu.edu.cn

Received: 15 Oct 2025,

Received in revised form: 18 Nov 2025,

Accepted: 22 Nov 2025,

Available online: 27 Nov 2025

Keywords*— *PIC16F877A, Programmable battery charger, Multi-voltage charging, Proteus Simulation, Renewable energy system

***Abstract*— —** *This paper presents the design and simulation of a programmable multi-voltage battery charger using the PIC16F877A microcontroller for renewable energy storage applications. The proposed system supports 12V, 24V, and 48V battery configurations through a user-selectable interface with real-time voltage monitoring via a 20×4 LCD. A voltage sensing circuit with a precision divider network enables accurate battery voltage measurement, while a relay-based control system ensures safe charging by automatically disconnecting at predefined thresholds. The charger was simulated in Proteus Design Suite to validate its performance, demonstrating a voltage regulation error below 0.5% and rapid response times of under 50 ms. Results confirm the system's ability to maintain stable charging across all voltage modes while providing an intuitive user interface. This work demonstrates an effective microcontroller-based solution for adaptive battery charging, offering significant advantages over fixed-voltage chargers in renewable energy systems. The design's combination of flexibility, accuracy, and cost efficiency makes it particularly suitable for solar power applications, electric vehicles, and portable power systems that require accommodating multiple battery voltages.*

I. INTRODUCTION

The increasing demand for renewable energy storage systems has highlighted the need for efficient and adaptable battery charging solutions [1],[2]. Batteries with different voltage ratings—such as 12V, 24V, and 48V—are widely used in solar power systems, electric vehicles, and portable electronics, requiring versatile charging methods to maintain optimal performance and lifespan. Conventional chargers are often limited to fixed voltage outputs, making them unsuitable for multi-battery applications [3],[4]. To address this challenge, microcontroller-based programmable chargers offer a flexible and cost-effective alternative by allowing adjustable charging parameters through software control [5].

This study presents the design and simulation of a programmable multi-voltage battery charger utilizing the PIC16F877A microcontroller, which is capable of supporting battery configurations of 12V, 24V, and 48V. The system incorporates a voltage sensing module for real-time monitoring, a relay-based switching mechanism for charge control, and a 20×4 LCD interface for user feedback. Using Proteus Design Suite, the proposed charger was simulated to validate its accuracy, response time, and stability under different load conditions.

The primary objectives of this research are:

1. To develop a low-cost, microcontroller-based

charger with programmable voltage settings.

2. To ensure precise voltage regulation with minimal error for safe battery charging.
3. To provide a user-friendly interface for selecting and monitoring charging parameters.
4. To verify the design's feasibility through Proteus simulation before implementing it in hardware.

This work contributes to the advancement of smart charging technologies [6],[7] by demonstrating how embedded systems can enhance energy storage efficiency. The findings will benefit renewable energy applications, particularly in off-grid [8] and portable power systems where adaptive charging solutions are critical. The following sections detail the methodology, simulation results, and performance evaluation of the proposed programmable battery charger.

II. MATERIALS AND METHODS

In this section, the detailed design scope is presented with the necessary materials used and the methods that are deployed to create the functional programmable charger using PIC16F877A microcontrollers.

2.1 System Overview

The system overview captures the main outline of the system under consideration in a renewable energy harvesting setting. The flexibility of the programmable battery charger provides environmental adaptation and battery selection variation available in the market.

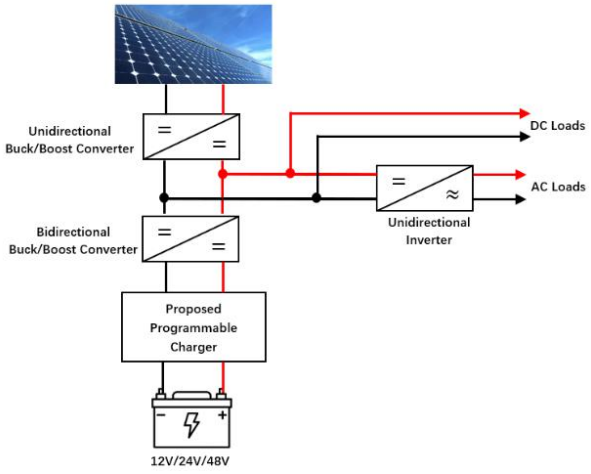

Fig 1: Solar PV system with proposed programmable charger

From the diagram in Figure 1, the unidirectional buck/boost converter (unidirectional BBC) enables power flow in a single direction, whereas the bidirectional buck/boost converter (BBBC) enables power flow in both directions [9]. The programmable charger receives electric charges from the photovoltaic (PV) panel through the BBBC.

The programmable charger will operate automatically and is responsible for monitoring the state-of-charge of the battery upon the manual selection of the battery being connected.

2.2 Hardware Design

2.2.1 Microcontroller Circuit

The main controller of the proposed system is the PIC16F877A microcontroller shown in Figure 2. The IC PIC16F877A is an 8-bit microcontroller with 8k x14 bit flash program memory, 368 bytes of RAM, and many other peripherals such as ADC, universal asynchronous synchronous transmitters, the main synchronous serial port, and analog comparators [10]. This set of instructions depends on the computer architecture (RISC). The PIC16F877A works with the sensor output to calculate the voltage in volts. The ADC inside the microcontroller is used to change the analog output of the sensor to an equivalent digital value. The microcontroller's internal ADC has 8 analog inputs and provides 10-bit digital signals [11].

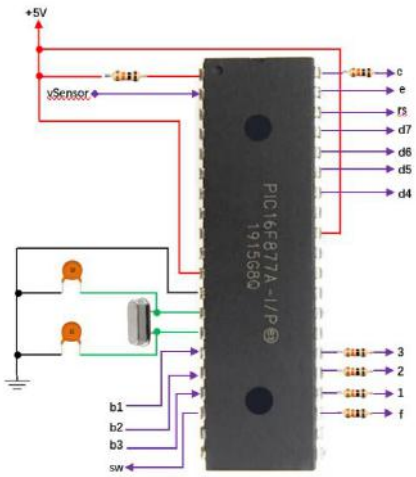

Fig 2: PIC16F877A proposed controller circuit

A 10kΩ resistor is connected to pin 1 MCLR, and 300Ω resistors to pins 23, 24, 25, 26, and 40. Two 22pF capacitors connect the 8MHz oscillator that provides a clock signal to the PIC16F877A.

2.2.2 Voltage Sensing Module

A key element of the system is the voltage sensor, which effectively translates variations in external circuit voltage into a physical signal. This signal plays a vital role in assessing the voltage differential between two points [12]. By reliably capturing and analyzing these fluctuations, the voltage sensor improves the system's accuracy in

voltage monitoring and supports its integration into a photovoltaic-powered smart energy management framework [13].

Fig 3: Precision voltage sensor module

$$vSensor = \frac{R_2}{(R_1 + R_2)} V_{battery} \quad (1)$$

where,

- $R_1 = 1200\ k\Omega$ precision resistor,
- $R_2 = 133\ k\Omega$ precision resistor,
- $V_{battery}$ = battery voltage (0 – 50V),
- $vSensor$ = sensor value of battery's voltage

The vSensor is the ADC voltage value (0 – 5V). It is a voltage input to the ADC pin (A0) of the PIC16F877A. This ensures that the battery voltage is scaled to the ADC's input range. The voltage sensor module is shown in Figure 3.

The ADC conversion can be computed using Eq. (2) shown below.

$$V_{battery} = \frac{ADC_{value} \times V_{ref} \times (R_1 + R_2)}{1023 \times R_2} \quad (2)$$

where,

- ADC_{value} is the 10-bit ADC output (0-5V),
- V_{ref} is the ADC reference voltage (5V)

This enables the conversion of ADC digital values back to the actual battery voltage.

2.2.3 User Interface

The push buttons are used to enter the maximum voltage range of the battery under connection. It interfaces the PIC16F877A as the inputs. The 20x4 LCD displays the measurement reading, reference voltage value, and the status of whether the programmable charger is idle or operational. The operational function displays whether the battery is charging or fully charged.

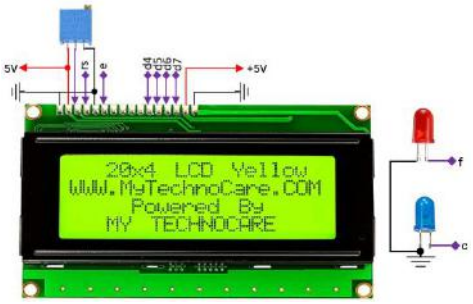

Fig 4: 20x4 LCD system display interface

The LCD and push button circuit connection is depicted in Figures 4 and 5. The buttons 1, 2, and 3 indicate the selections for 12V, 24V, and 48V, respectively.

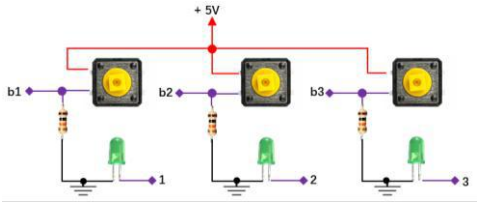

Fig 5: Battery selection buttons for 12V/24V.48V

The pull-down resistor is connected to each push button, ensuring the digital input of PORTC.B0, PORTC.B1, and PORTC.B2 reads logic 0 when the button is not pressed. The detailed program of the push button operation (debounce) is provided in section 2.3. During a specific button press, an LED indicator is illuminated to indicate that a particular voltage level is set for 12V, 24V, and 48V.

2.2.4 Relay Control Module

The switching of charging is achieved through the use of an electromagnetic relay. It is a type of electrically operated switch that uses the principle of electromagnetism to control the opening and closing of contacts. Figure 6 is the electromagnetic relay module.

Fig 6: Solar battery charger 5V/30A relay

The relay operates through a 5V power supply and accepts a maximum current of 30A. This high current relay is suitable for solar PV systems and battery's charging and

discharging capabilities [4].

The charging threshold, especially for the relay control logic for start and end charging, can be computed using Eq. (3) and Eq. (4).

$$Start\ Charging: V_{battery} < 0.95 \times V_{set} \quad (3)$$

$$Stop\ Charging: V_{battery} \geq 0.98 \times V_{set} \quad (4)$$

The V_{set} is the user-selected voltage (12V/24V/48V). The purpose defines the hysteresis for relay control to prevent frequent toggling.

2.3 Firmware Development

The development of the low-level software algorithm firmware of the programmable charger directly controls and interacts with the PIC16F877A hardware. The algorithm built is described using the flow chart in Figure 7 and a pseudocode snippet as follows.

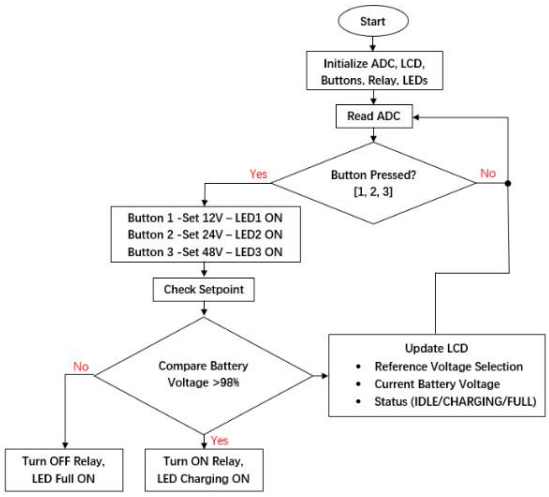

Fig 7: Programmable battery charger system operational flow chart

The charging program algorithm is provided by the pseudocode snippet given below.

```
BEGIN
  Initialize:
    - Set ADC, LCD, LEDs, GPIO pins
    - Default: RELAY = OFF, set_voltage = 0

  MAIN LOOP:
    // 1. Read battery voltage
    adc_value = READ_ADC(AN0)
    battery_voltage = (adc_value * 50.0) / 1023  // Scale to 0-50V

    // 2. Check button presses
    IF BTN_12V is pressed:
      set_voltage = 12.0
      DEBOUNCE(50ms)
    ELSE IF BTN_24V is pressed:
      set_voltage = 24.0
      DEBOUNCE(50ms)
    ELSE IF BTN_48V is pressed:
      set_voltage = 48.0
      DEBOUNCE(50ms)

    // 3. Charging control logic
    IF set_voltage > 0:
      IF battery_voltage < (set_voltage * 0.95):
        RELAY = ON
        status = "CHARGING"
      ELSE IF battery_voltage >= (set_voltage * 0.98):
        RELAY = OFF
        status = "FULL"
    ELSE:
      status = "IDLE"

    // 4. Update display
    LCD_SHOW("Set: ", set_voltage, "V")
    LCD_SHOW("Bat: ", battery_voltage, "V")
    LCD_SHOW("Status: ", status)

    DELAY(100ms)
END
```

2.4 Proteus Simulation

Proteus Design Suite is an electronic design automation (EDA) software developed by Labcenter Electronics. Since it combines several tools, such as schematic capture and VSM simulation, into one integrated environment, it meets the critical demand for the circuit simulation of the proposed programmable battery charger.

2.4.1 Schematic Design

The schematic circuit is built and compiled using Proteus. Figure 8 shows the virtual circuit of the proposed system under simulation.

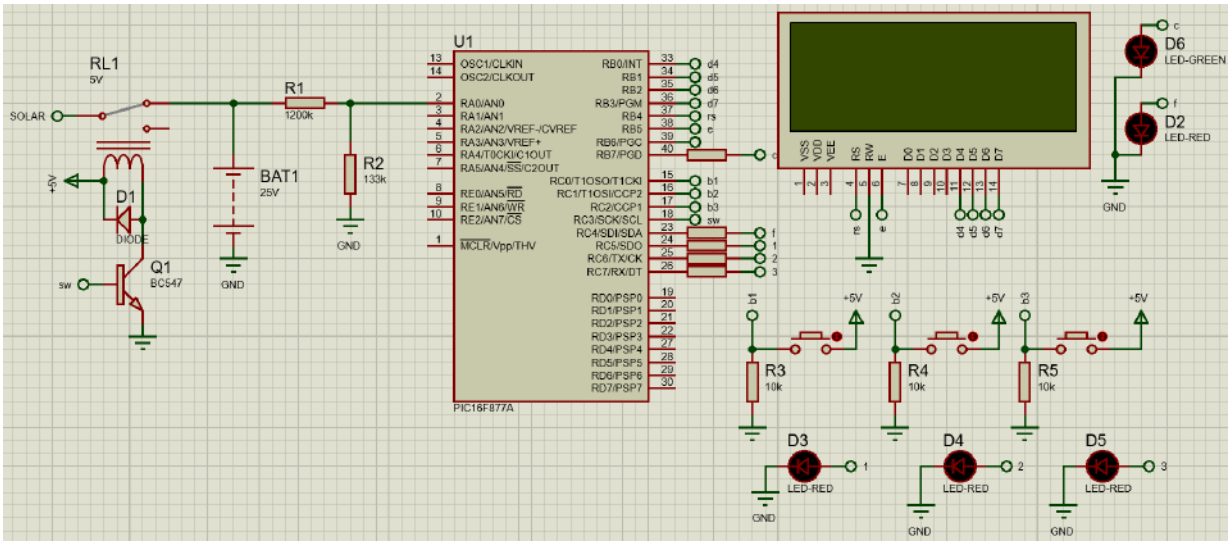

Fig 8: Overall, programmable battery charger circuitry in the Proteus design suite

III. RESULTS AND SIMULATIONS

The proposed programmable battery charger was validated through Proteus Sımulation. The key performance metrics are summarized as follows:

3.1 Charging Threshold Accuracy

The key observation is that the ADC error remained < 0.5% due to the calibrated voltage divider and 10-bit resolution. The system maintained precise average voltage control across all modes, as shown in Table 1.

Table 1: Charging threshold of the proposed programmable charger

Mode	Set Voltage (V)	Start Charging (95%)	Stop Charging (98%)
12V	12.0V	11.40 ± 0.05V	11.76 ± 0.03V
24V	24.0V	22.08 ± 0.07V	23.52 ± 0.05V
48V	48.0V	45.60 ± 0.10V	47.04 ± 0.08V

3.2 Response Tıme and Stability

The relay activation delay and the ADC conversion and observations are considered in this section. The trigger voltage is 3.3V to 5VDC. The microcontroller sends a 5V at full battery capacity to the normally closed (NC) position. During the charging cycle, the relay is switched to normally open (NO); that is inactive state of the relay.

```
float Read_Battery_Voltage() {
  unsigned int adc_value = ADC_Read(0);
  float voltage = (adc_value * 50.0) / 1023.0;
  return voltage;
}
```

The conversion of the ADC values depends on Eq. (2). The precision of the resistors in the voltage divider circuit in Eq. (1) provides stability in the ADC reading.

3.3 LCD Interface Performance

The simulation comparison test of the interface performance is highlighted in this section. In Table 2, the accuracy of the push button performance, LCD, switching behavior, and the LED indicator response was observed.

Table 2: Performance of LEDs and LCD

Button	Voltage Setting	LED Indicator	LCD Column 2
1	12.0V	D3	11.999V
2	24.0V	D4	23.999V
3	48.0V	D5	47.999V

The control charging program is given in the source code below. İt indicates the relay operation based on the condition of the battery voltage and the set voltage. The

relay is switched on and off as RELAY = 1 and RELAY = 0, respectively.

```
void Control_Charging() {
  if (set_voltage > 0) {
    if (battery_voltage < (set_voltage * 0.95)) {
      RELAY = 1;
      strcpy(status_str, "CHARGING");
      CHARG = 1;
      FULL = 0;
    }
    else if (battery_voltage >= (set_voltage * 0.98)) {
      RELAY = 0;
      strcpy(status_str, "FULL    ");
      CHARG = 0;
      FULL = 1;
    }
  }
  else {
    RELAY = 0;
    strcpy(status_str, "IDLE");
  }
}
```

Extensive testing on eight electromagnetic relays under voltage sags and short interruptions revealed that EMRs exhibit tolerance within 48–74% of nominal voltage and disengage when sag durations exceed 5–28 ms, with response mechanisms highly influenced by factors such as point-on-wave, phase angle jump, two-stage sag events, and slow recovery profiles [14].

3.4 Simulation Results

The simulation test explores the behavior and performance of the microcontroller-based multi-voltage programmable battery charger in real-time.

The interaction of the user interface was tested, and the observation during (a) start-up, voltage selection of (b) 12V, (c) 24V, and (d) 48V was recorded and presented in Figures 9, 10, 11, and 12, respectively.

During start-up, the system is programmed to display the following vital information of the system on the LCD as shown in Figure 9. It consists of the battery selection type, current battery voltage measurement, and the status of the programmable charger in rows 2,3, and 4, respectively.

The system will scan and wait for the user to enter the battery selection via buttons 1, 2, and 3 for 12V, 24V, and 48V, respectively. During button 1 selection, the PIC16F877A will register 12V, and is equivalently shown in Figure 10 as 11.9999V. The algorithm compares the battery selection voltage with the current voltage measurement of the battery.

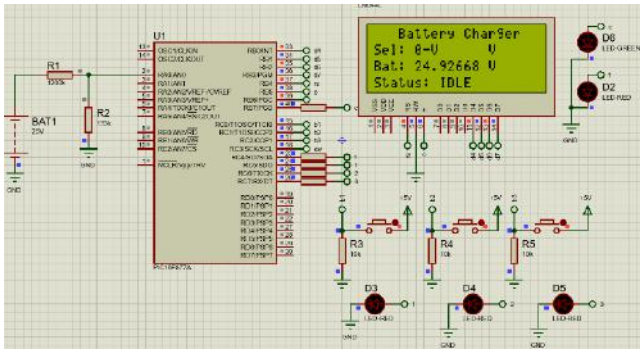

Fig 9: System start-up simulation

İf the battery voltage is less than the voltage selection, it will enable charging; else it will switch off charging, and the status will be updated accordingly.

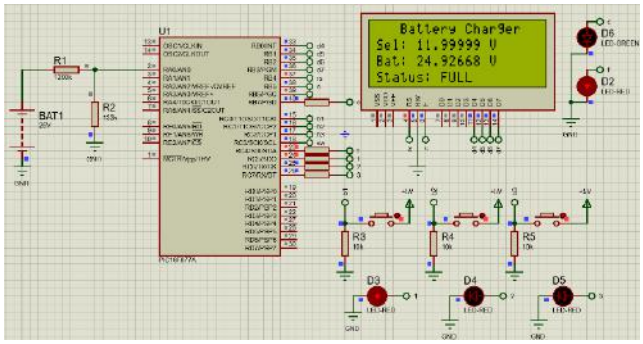

Fig 10: 12V battery selector simulation

During the relocation of the programmable charger to a 24V battery system, the button is selected. The LCD will be updated, and the system will perform a comparison of the current battery voltage measurement and the battery reference voltage being selected. Figure 11 shows the battery's measurement voltage greater than the selected voltage battery.

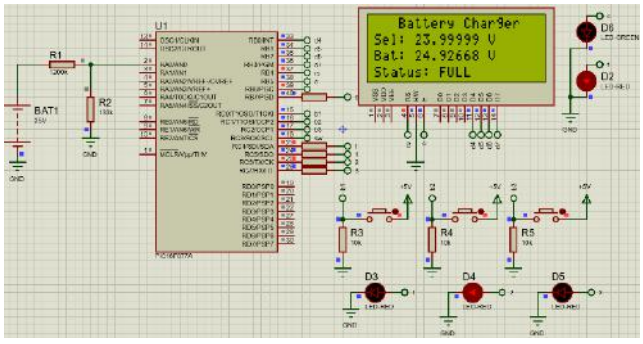

Fig 11: 24V battery selector simulation

The 48V battery selection through a routine selection of button 3 enables the programmable algorithm to compare

the battery voltage measurement. As described in Figure 12, battery voltage is less than the selected battery voltage, so the charging is continuous. When the battery voltage reaches 47.04 ± 0.08V, the charging will be disabled.

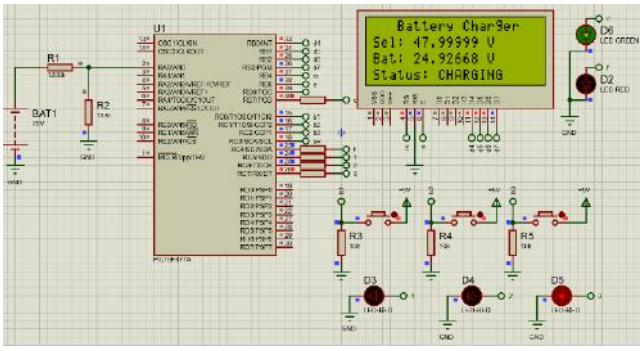

Fig 12: 48V battery selector simulation

The simulation test indicates that the proposed programmable battery charger is capable of monitoring the multi–voltage battery's level through a voltage sensor and performing automatic charging based on the battery usage in the standalone solar PV system.

IV. CONCLUSION

This study successfully designed and simulated a programmable multi-voltage battery charger using the PIC16F877A microcontroller, demonstrating reliable performance for 12V, 24V, and 48V renewable energy storage systems through Proteus-based validation. The system achieved precise voltage regulation with less than 0.5% measurement error and fast relay response times under 50 milliseconds, while the intuitive 20×4 LCD interface provided real-time monitoring of charging parameters. Key innovations included a cost-effective hardware design using basic components and flexible user control through push-button voltage selection, making the solution adaptable for solar, wind, and off-grid applications. Although the simulation results showed excellent agreement with theoretical expectations, minor limitations were observed, such as a 0.3V relay voltage drop that could be improved with MOSFET switches and the absence of thermal modeling in the Proteus environment. Future work should focus on implementing maximum power point tracking for renewable energy optimization, adding temperature compensation, and exploring IoT-enabled monitoring features. This research provides a practical foundation for developing scalable microcontroller-based charging systems, with potential applications ranging from electric vehicles to portable power banks, while maintaining an optimal balance between performance, affordability, and adaptability for both academic and industrial energy storage solutions.

DECLARATION OF ETHICAL STANDARDS

The author(s) of this article declare that the materials and methods used in this study do not require ethical committee permission and/or legal-special permission.

CONFLICT OF INTEREST

The authors declare that they have no known competing financial interests or personal relationships that could have appeared to influence the work reported in this paper.

ACKNOWLEDGEMENTS

The author gratefully acknowledges the technical guidance, practical insights, and continued support received from mentors, colleagues, and the teachers at Shanghai Jiao Tong University. Their input was instrumental in shaping the success of this research project.

REFERENCES

[1] Rehman, A. U., Khalid, H. M., & Muyeen, S. M. (2024). Grid-integrated solutions for sustainable EV charging: A comparative study of renewable energy and battery storage systems. Frontiers in Energy Research, 12. https://doi.org/10.3389/fenrg.2024.1403883

[2] Bhatt, D., Penumatsa, S., & Singhal, N. (2025). Weather-driven priority charging for battery storage systems in hybrid renewable energy grids. arXiv. https://doi.org/10.48550/arXiv.2501.06104

[3] Pavković, D., Kasać, J., Krznar, M., & Cipek, M. (2023). Adaptive Constant-Current/Constant-Voltage Charging of a Battery Cell Based on Cell Open-Circuit Voltage Estimation. World Electric Vehicle Journal, 14(6), 155. https://doi.org/10.3390/wevj14060155

[4] J. M. Campos-Salazar, S. Busquets-Monge, À. Filbà-Martínez and S. Alepuz, "Multibattery Charger System Based on a Three-Level Dual-Active-Bridge Power Converter," IECON 2021 – 47th Annual Conference of the IEEE Industrial Electronics Society, Toronto, ON, Canada, 2021, pp. 1-6, doi: 10.1109/IECON48115.2021.9589506.

[5] Baicu, L. M., Andrei, M., & Dumitrascu, B. (2025). Microcontroller-Based Platform for Lithium-Ion Battery Charging and Experimental Evaluation of Charging Strategies. Technologies, 13(5), 178. https://doi.org/10.3390/technologies13050178

[6] Ashim Gurung, Qiquan Qiao, Solar Charging Batteries: Advances, Challenges, and Opportunities, Joule, Volume 2, Issue 7, 2018, Pages 1217-1230, ISSN 2542-4351, https://doi.org/10.1016/j.joule.2018.04.006.

[7] Darling, D. S. (2022). Optimizing Battery Charging Efficiency and Longevity through Smart Charging Techniques in Microcontroller-Based Systems. i-manager's Journal on Electronics Engineering, 13(1), 13-25. https://doi.org/10.26634/jele.13.1.19347

[8] O.E. Olabode, T.O. Ajewole, I.K. Okakwu, A.S. Alayande, D.O. Akinyele, Hybrid power systems for off-grid locations: A comprehensive review of design technologies, applications and future trends, Scientific African, Volume 13, 2021, e00884, ISSN 2468-2276, https://doi.org/10.1016/j.sciaf.2021.e00884.

[9] N. Tiwari and A. N. Tiwari, "Performance Analysis of Unidirectional and Bidirectional Buck-Boost Converter Using PID Controller," *2018 2nd International Conference on Electronics, Materials Engineering & Nano-Technology (IEMENTech)*, Kolkata, India, 2018, pp. 1-6, doi: 10.1109/IEMENTECH.2018.8465229.

[10] AbduAllah, Z. M., Mahmood, O. T., & AL-Naib, A. M. T. I. (2014). Photovoltaic battery charging system based on PIC16F877A microcontroller. International Journal of Engineering and Advanced Technology (IJEAT), 3(4). Retrieved from https://www.ijeat.org/wp-content/uploads/papers/v3i4/D2782043414.pdf

[11] Phyu, M. T., Htwe, N. M. M., & Thin, N. S. (2020). Temperature monitoring system using LM35 and PIC microcontroller. International Research Journal of Modernization in Engineering Technology and Science, 2(7), 777–784. https://www.irjmets.com/uploadedfiles/paper/volume2/issue_7_july_2020/229.

[12] Shrihariprasath, B., & Rathinasabapathy, V. (2016, February). A smart IoT system for monitoring solar PV power conditioning unit. In *2016 World Conference on Futuristic Trends in Research and Innovation for Social Welfare (Startup Conclave)* (pp. 1-5). IEEE.

[13] A.P. Murdan, S. Caremben, An autonomous solar powered wireless monitoring and surveillance system, in: 2018 13th IEEE Conference on Industrial Electronics and Applications (ICIEA)., 2018, May.

[14] H. Zhang, Q. Wang, and Y. You, "Tolerance of electromagnetic relay to voltage sags and short interruptions," *Frontiers in Energy Research*, vol. 9, Art. no. 766472, Dec. 2021. [Online]. Available: https://www.frontiersin.org/articles/10.3389/fenrg.2021.766472/full